

Spiral-pattern formation and multistability in Landau-Ginzburg systems

J. A. Tuszynski and M. Otwinowski

Department of Physics, University of Alberta, Edmonton, Alberta, Canada T6G 2J1

J. M. Dixon

Department of Physics, University of Warwick, Coventry, CV4 7AL, United Kingdom

(Received 16 April 1991)

This paper is concerned with the formation of spiral patterns in a broad range of physical, chemical, and biomolecular systems. An overview of a series of experiments is presented followed by an analysis of spiral reductions for several types of Landau-Ginzburg equations which are applicable to these examples. The main result here is that spiral patterns occur as *exact* solutions of the highly nonlinear order-parameter equations of motion under three types of conditions: first, at criticality; second, at tricriticality; and third, in the presence of special types of defects which we have modeled with a nonautonomous term. A particularly timely application to ferromagnetic thin films is discussed and provides a physical interpretation of the spiral domain structures found experimentally to arise there.

I. INTRODUCTION

This paper has been motivated by the observation of an ever increasing number of spiral and helical patterns being formed in a wide range of physical, chemical, and biomolecular systems. An example of spiral structures, well known for many years, occurs in crystal growth.¹ In fully developed crystals structural defects take various forms including the so-called screw dislocation, which falls into the category discussed in the present paper. One of the most interesting examples of unusual defects are the newly discovered curling crystals which form a spiral staircase in a vial. Interestingly, these spirals are always counterclockwise and the patterns are highly reproducible.² However, it is less well known that spiral and helical phases and domains can be observed in a number of magnetic systems. For example, in some rare-earth metals and their compounds helical antiferromagnetism has been found as an equilibrium ordered state.³ The growth of spiral magnetic domains has been recently observed to occur under nonequilibrium conditions and is associated with fascinating physical phenomena.⁴ These experiments⁴ involved epitaxially grown single-crystal garnet ferrite films of the material $(Y,Sm)_3(Fe,Ga)_5O_{12}$. These authors demonstrated⁴ that, when subjected to an alternating square magnetic field, with a finely tuned amplitude, the ferrite films exhibit the formation of macroscopic spiral domains with remarkably long lifetimes of the order 10 s. These structures appeared to have soliton like qualities, with respect to their spatial identity and form, and they were thermodynamically metastable. A preliminary theoretical discussion of this phenomenon can be found elsewhere.⁵ Another recent paper⁶ reported the formation of spiral domains in single iron garnet films subjected to a *static* magnetic field, in a narrow magnitude range. The process of spiral domain formation appears to be very sensitive to the physical properties of the films and to the presence of de-

fects.

In their most recent study, Kandaurova and Sviderskii⁷ found a most intriguing formation of quasiperiodic lattices composed of spiral domains. We will address the question of ensembles of spiral domains, and especially their size fluctuations later in this paper. It should be pointed out, however, that the spiral magnetic domains had been seen in Permalloy-coated garnets some ten years earlier.⁸ Furthermore, this earlier publication⁸ indicates that spirals are related to concentric circles of magnetization and both of these types of structure may originate from magnetic bubbles. A possible theoretical explanation of this effect is based on the definition of topological charge. Since cholesteric order in liquid crystals exhibits many similarities with helical antiferromagnetism⁹ it is conceivable that spiral patterns may, in the future, be detected in liquid crystalline systems under nonequilibrium conditions. A series of experiments carried out by Joets and Ribotta demonstrated that the application of an external *electric* field is capable of producing dramatic structural changes leading to pattern formation cascading eventually to chaos.

Spiral patterns are also well known to appear in oscillating reaction-diffusion systems i.e., in chemical waves (sometimes called Winfree waves¹¹) associated with various types of reactions^{12(a)}. A recent series of papers¹² have reported the observation of spiral waves in an excitable medium, of a particular chemical composition, which exhibit interesting dynamical behavior. In particular, it has been shown that a pair, consisting of a spiral and a counterspiral, collide to produce a vortexlike nearly spherical structure^{12(b)}.

In the last few years spiral patterns have been observed in the hysteretic turbulence of Taylor-Couette flows where the regions of laminar and turbulent flow coexist and each of which is confined to a spiral shaped region within a rotating cylinder.¹³ In an up-to-date monograph^{14(a)}, a section has been devoted to the various

occurrences of spiral waves in a variety of biological, physiological, and chemical systems. Electrochemical waves in the brain tissue, propagation of signaling patterns in slime mold, and waves propagating in the heart muscle (associated with cardiac arrhythmias) are a few of the examples cited.^{14(a)} Furthermore, spiral modes with a definite range of stability have been experimentally observed in the dynamics of premixed flames.¹⁵

It has been observed¹² that when a spiral and a counterspiral, with the same magnitude of topological charge, collide, they may annihilate each other and form a circular pattern (see Fig. 1). In this connection, in a theoretical paper¹⁶ on the effects of magnetic-field penetration in superconductors it has been demonstrated how spiral-like superconducting order parameters and magnetic vector potentials may arise very close to the superconducting temperature. They may be interpreted as preceding vortex formation as the temperature is lowered. Numerical simulations for reaction-diffusion models indicate that spiral waves may evolve in a natural way from plane waves.^{14(b)} Belousov-Zhabotinskii reactions give experimental support to these predictions (see Fig. 2). Tyson and Keener¹⁷ have recently written an extensive review on traveling waves in excitable media with a large part of it discussing the origin and properties of spiral waves in reaction-diffusion systems. The reader is referred to this paper for consultation concerning chemical reactions. A related phenomenon of the emergence of helical organizing centers in excitable media has been reviewed by Henze, Lugosi, and Winfree.¹⁸

These are but a few examples of the areas in which equations, describing the various nonhomogeneous phenomena related to multistability, may be applied and appropriate particular solutions with spiral geometry may be found. We also see striking analogies to these condensed matter phenomena in such disparate areas as cosmology (spiral galaxy formation)¹⁹ and biophysics (spiral arrangements of cell microtubules²⁰).

Our belief is that these diverse phenomena, which are seemingly unrelated, have indeed a unifying physical basis. We will attempt to demonstrate this to the reader in the present paper. To keep the discussion at a sufficiently simple and yet fairly general level we will adopt the Landau-Ginzburg approach²¹ to the modeling of systems under consideration.

II. SPIRAL ORDER PARAMETERS

A large class of many-body systems composed of Bose-Einstein or Fermi-Dirac particles can be described

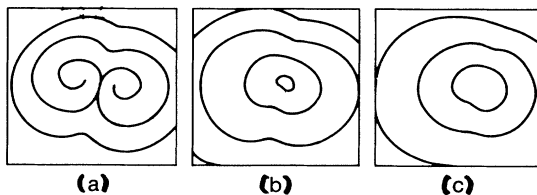


FIG. 1. Collision of a spiral with a counterspiral following Ref. 12.

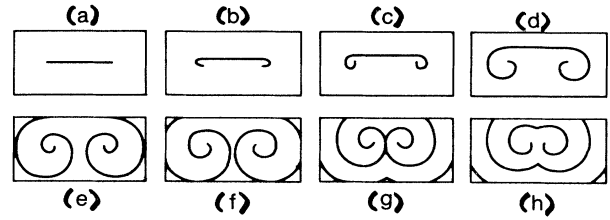


FIG. 2. Evolution of a pair of spirals from a plane wave following Ref. 14(b).

using an effective second-quantized Hamiltonian of the type

$$H_{\text{eff}} = \sum_{k,l} \omega_{k,l} a_k^\dagger a_l + \sum_{k,l,m} \Delta_{k,l,m} a_k^\dagger a_l^\dagger a_m a_{k+l-m}, \quad (1)$$

where a_k (a_k^\dagger) are annihilation (creation) operators. Many theoretical approaches to the analysis of this type of Hamiltonian have been proposed and utilized in the past, e.g., the Green function method, Feynmann diagrammatic techniques, or other methods of quantum field theory. However, an approach has just been developed²² to convert this problem to one of nonlinear differential equations describing the time evolution of the associated quantum field operator and which for systems with a large number of particles is virtually exact. It has been demonstrated in these papers²² that the classical part Φ of the quantum field Ψ plays a very similar role to that of an order parameter. The latter quantity was introduced some 50 years ago by Landau²¹ and, in itself, constituted a breakthrough in the understanding of critical phenomena. It was, however, considered to be entirely phenomenological for many years. The method of coherent structures,²² however, clearly shows that this is not the case and that there is a much more general and fundamental origin of both the order parameter and the Landau-Ginzburg (LG) Hamiltonian density,

$$H_{\text{LG}} = D |\nabla \Phi|^2 + A_2 |\Phi|^2 + A_4 |\Phi|^4 + \dots \quad (2)$$

It transpires that the standard method of minimizing the LG Hamiltonian functional is indeed equivalent to the equation of motion of the order-parameter field obtained from the effective Hamiltonian in Eq. (1). It should be pointed out that, for a particular physical system, namely standard superconductors Gor'kov²³ showed a similar relationship between the BCS Hamiltonian [which is an example of our Eq. (1)] and the LG picture.

In a later part of this paper we shall explicitly demonstrate how spiral solutions can be obtained for a number of nonlinear partial differential equations (PDE's) describing the dynamics of order-parameter fields. The method used in these calculations is called the symmetry reduction method²⁴ and, without going into detail, it relies on finding a so-called symmetry variable ξ , such that the classical order parameter Φ takes the form

$$\Phi(x, y, z, t) = \rho(x, y, z) F(\xi). \quad (3)$$

Here, ρ plays the role of a spatially dependent damping

factor while F satisfies an ordinary differential equation (ODE) obtained by reduction from the original PDE. Among the many possible symmetry variables, ξ , one often finds spiral and helical variables which provide exact reductions under a specific set of circumstances to be discussed later. The general form of spiral and helical symmetry variables is

$$\xi = \Omega(z, t) \pm m\theta + \sigma(r), \quad (4)$$

where $r^2 = x^2 + y^2$ and the function $\Omega(z, t)$ is the velocity of rotation of the pattern, m is the number of arms on the spiral, which defines the so-called topological charge,^{14(a)} and $\sigma(r)$ is a radial function in two dimensions whose specific form describes the type of spiral which may occur. For example, $\sigma = a(r - r_0)$ for an Archimedian spiral (where a and r_0 are constants) whereas $\sigma = a \ln(r - r_0)$ denotes a logarithmic spiral. In Fig. 3 we have illustrated how the topological charge affects the number of arms and helicity.

III. EQUATIONS OF MOTION AND SPIRAL REDUCTIONS

In this section a survey will be provided of some of the most important PDE's in the description of multistable systems which are characterized by the presence of spiral symmetry variables. The theoretical framework used is that of LG formalism but several distinct cases will be discussed, i.e., Hamiltonian versus free energy descriptions and real versus complex order parameters. The mathematical approach to the relevant equations of motion is the method of symmetry reduction.²⁴ This method makes use of continuous Lie symmetries of the original PDE in order to find dependent and independent variables which will reduce the PDE to an equation one order less. Often, it will transpire that the result is an ODE in the variables. Within the class of reductions to ODE's numerous distinct possibilities occur simultane-

ously. Since, in general, these types of equation, which we are interested in, possess translational and rotational symmetries quasilinear, cylindrical, and spherical solutions are found to exist in all cases. However, under special circumstances, when the nonlinearity takes the form of a monomial in the order parameter, scale invariant symmetry of the equation results in the creation of a large number of classes of exact solutions.²⁵ One such class very often contains *spiral solutions*. The conditions required for nonlinear terms to reduce to a monomial can be physically interpreted as implying that the system is either in the vicinity of the critical or tricritical points. In the remainder of this section we shall discuss the individual cases.

Within the LG formalism there appear to be two main approaches to investigate the dynamics of critical systems. The first one is based on a Hamiltonian or Lagrangian density while the second is a "phenomenological" free energy expansion.

A. The nonlinear Klein-Gordon equation (NLKGE)

We can write an LG Hamiltonian density which includes potential energy, a Ginzburg $(\nabla\Phi)^2$ term describing inhomogeneities, as well as a kinetic energy contribution, in the following general form:

$$H_1 = \frac{1}{2}m(\Phi_t)^2 + \frac{1}{2}D(\nabla\Phi)^2 + A_2\Phi^2 + A_4\Phi^4 + A_6\Phi^6. \quad (5)$$

In Eq. (5), Φ is a real order parameter and $A_2 = \alpha(T - T_c)$ where T denotes temperature and α is a constant, the critical temperature being written as T_c . The associated transition is of second order if $A_4 > 0$ and takes place at $T = T_c$. It is of first order when $A_4 < 0$ and occurs at $T_c^* = T_c + A_4^2/4\alpha A_6$. The kinetics of the transitions may be obtained by minimizing the Hamiltonian function with respect to Φ to give the Euler-Lagrange equations, which result in the real non-linear Klein-Gordon equation.

$$\square_\epsilon \Phi = -2(A_2\Phi + 2A_4\Phi^3 + 3A_6\Phi^5) \equiv F(\Phi), \quad (6)$$

where the symbol \square_ϵ is defined by

$$\square_\epsilon = \frac{\partial^2}{\partial x_0^2} + \epsilon \sum_{i=1}^3 \frac{\partial^2}{\partial x_i^2}, \quad (7)$$

and ϵ is a signature given by $\epsilon = -\text{sgn}(D)$. The independent variables in Eq. (7) are defined by

$$x_0 = m^{-1/2}t \quad \text{and} \quad (x_1, x_2, x_3) = |D|^{-1/2}(x, y, z). \quad (8)$$

First, in the case of cubic nonlinearity in Eq. (6) i.e., for $A_2 = A_6 = 0$, corresponding to the critical point $T = T_c$, a spiral type of reduction is found²⁶ as

$$\Phi = \rho F(\xi), \quad (9)$$

where

$$\rho = 2B[(4A_4/|D|)(B^2 + 4)r^2]^{-1/2}, \quad (10)$$

and $r = (x_1^2 + x_2^2)^{1/2}$. The symmetry variable ξ is given by

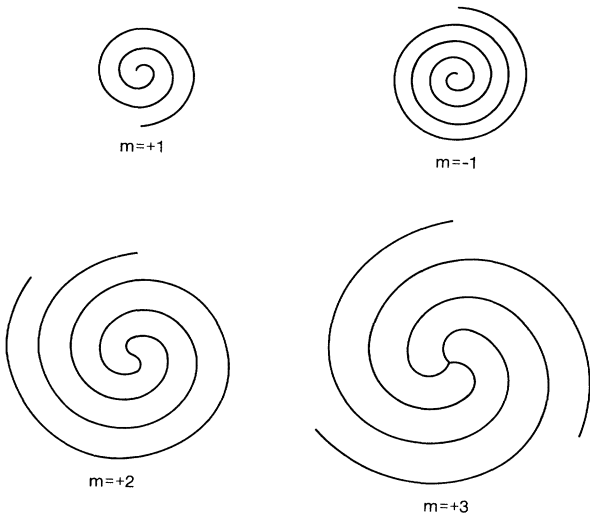


FIG. 3. Schematic illustrations of spirals with various topological charges m .

$$\xi = [4B/(B^2+4)][-(B/2)\ln r + \theta]. \quad (11)$$

The angle θ in Eq. (11) is defined by

$$\theta = \tan^{-1}(x_2/x_1), \quad (12)$$

and B is an arbitrary nonzero constant. A constant value of ξ describes a logarithmic spiral. The reduced ODE for F takes the form of an anharmonic dissipative oscillator equation

$$F'' + F' + \frac{B^2+4}{4B^2}F + F^3 = 0. \quad (13)$$

This has been extensively analyzed in a separate publication²⁷ and, in order to assist the reader, we have summarized its analytical solutions in the Appendix.

Secondly, for quintic nonlinearity in Eq. (6), spiral solutions emerge from symmetry reduction only at a particular point on the phase diagram, i.e., the tricritical point defined by $A_2 = A_4 = 0$, at which a line of first-order transitions intersects a line of second-order ones. The spiral solution found here is²⁸ in the form of Eq. (9) where

$$\rho = \left[\frac{6A_6}{|D|} \frac{B^2+1}{B^2} r^2 \right]^{-1/4} \quad (14a)$$

and

$$\xi = -\frac{B}{B^2+1}(B \ln r + \theta) \quad (14b)$$

The reduced ODE, in this case, becomes

$$F'' + F' + \frac{B^2+1}{4B^2}F + F^5 = 0. \quad (15)$$

Equation (15) is also in the form of a damped anharmonic oscillator and particular solutions can be found in the Appendix but are not as numerous as those known for the cubic case.

B. The nonlinear Schrödinger equation (NLSE)

For complex order parameters Φ and defining the conjugate momentum as

$$\pi = \frac{-i}{2}\Phi^*, \quad (16)$$

a more convenient approach is through Euler-Lagrange equations obtained from the Lagrangian functional²⁹

$$L = \frac{i}{2}(\Phi\Phi_t^* - \Phi^*\Phi_t) - \frac{D}{2}|\nabla\Phi|^2 - A_2|\Phi|^2 - A_4|\Phi|^4 - A_6|\Phi|^6, \quad (17)$$

where we have assumed that the effective mass of the system is negligible. The resultant equation of motion for the order-parameter field takes the form of a nonlinear Schrödinger equation given by

$$-i\Phi_t = D\nabla\Phi + 2A_2\Phi + 4A_4|\Phi|^2\Phi + 6A_6|\Phi|^4\Phi. \quad (18)$$

This equation has been the subject of a symmetry reduction analysis carried out by Gagnon and Winternitz.³⁰

Among the reductions found for the NLSE, Eq. (18), one also finds spiral-like solutions, namely

$$\xi = B \ln r + \theta, \quad (19)$$

where the order parameter Φ is given by

$$\Phi = \alpha[\exp i\chi(\xi)]F(\xi). \quad (20)$$

In Eq. (20)

$$\alpha = r^{-\delta} \exp[i(2A_2t)], \quad (21)$$

and χ is defined by

$$\chi = S_0 \int F^{-2} \exp[2\delta\xi B/(B^2+1)] d\xi. \quad (22)$$

Here, $\delta = \frac{1}{2}$ when $A_4 = 0$ and $\delta = 1$ when $A_6 = 0$. The remaining constants B and S_0 are arbitrary. D in Eq. (18) has been set equal to unity through an appropriate scaling. The reduced ODE for F is³⁰

$$(B^2+1)F'' - (B^2+1)F^{-3} \exp[4\delta B\xi/(B^2+1)] S_0^2 - 2\delta B F' + \delta^2 F = -n A_n F^{n-1}, \quad (23)$$

where $n = 4$ or 6 in the two cases considered, respectively.

C. The time-dependent Landau-Ginzburg equation (TDLGE)

The second type of approach used in LG modeling is based on a free energy density expansion

$$G = \frac{1}{2}D(\nabla\Phi)^2 + A_2\Phi^2 + A_4\Phi^4 + A_6\Phi^6, \quad (24)$$

where G is the free energy density. The relaxation kinetics of the order parameter Φ can be described by the TDLGE obtained by minimizing the free energy functional. This is obtained through an Onsager evolution equation $\partial\Phi/\partial t = \delta G/\delta\Phi$ as

$$\Phi_t + \nabla^2\Phi = a_2\Phi + a_4\Phi^3 + a_6\Phi^5. \quad (25)$$

We have scaled the time in (25) as well as polynomial coefficients by

$$t \rightarrow -\beta\Gamma \frac{Dt}{2}, \quad a_2 = \frac{2A_2}{D}, \quad (26)$$

$$a_4 = \frac{4A_4}{D}, \quad a_6 = \frac{6A_6}{D}.$$

Here “ \rightarrow ” indicates that t is scaled, $\beta = (k_B T)^{-1}$ and Γ is a phenomenological damping coefficient. Therefore, this is a macroscopic thermodynamic approach which is strictly applicable to globally nonconserved order parameters. Steady-state patterns are readily obtained from Eq. (25) by simply setting $\Phi_t = 0$. A series of papers³¹ have been devoted to a complete analysis of the TDLGE using the symmetry reduction method. Not surprisingly, spiral solutions have again been found to exist both at criticality and tricriticality. In the first case, i.e., when $A_2 = A_6 = 0$ this procedure yields, in the same form as Eq. (9),

$$\rho = \left[\frac{4B^2}{|a_4|(B^2+1)r^2} \right]^{1/2} \quad (27a)$$

and

$$\xi = \frac{-2B}{B^2+1} \left[-\frac{1}{2}B \ln r + \theta \right]. \quad (27b)$$

At the tricritical point, when $A_2 = A_4 = 0$ it is found, in a similar way,

$$\rho = \left[\frac{4B^2}{|a_6|(B^2+1)r^2} \right]^{1/4} \quad (28a)$$

and

$$\xi = \frac{-2B}{B^2+1} (B \ln r + \theta). \quad (28b)$$

The reduced equation in both cases takes a similar form which may be written as

$$F'' + F' + \frac{B^2+1}{4B^2} F + \epsilon F^{n-1} = 0, \quad (29)$$

where $\epsilon = -\text{sgn}(a_4)$ for $n=4$ and $\epsilon = -\text{sgn}(a_6)$ in the case when $n=6$. Equation (29) is also an example of the damped anharmonic oscillator equation, some special solutions for which may be found in the Appendix.

In summary, we have shown that spiral order-parameter structures arise in a natural way as *exact* solutions of several important classes of equations of motion for multistable critical systems. It should be pointed out, however, that the conditions on their existence require either the system to be precisely at the critical point or at the tricritical point. This may in fact mean that these types of structure originate in the immediate vicinity of these points on the phase diagram. In fact, Greenberg³² demonstrated the existence of periodic spiral solutions to multidimensional LG-type equations. They may exist as approximate solutions in the vicinity of these points provided they are stabilized. This possibility may be brought about, first of all, by the conservation of topological charge which has to be upheld as long as two spirals of opposite helicity do not collide or come together in too close a proximity. Thermal fluctuations may have an effect on the size and shape of the spirals but do not necessarily have to annihilate them. Finally, the presence of structural defects in the sample may contribute in a positive way, and indeed to the onset of their existence.¹⁸ There is another interesting aspect of spiral and helical stability, i.e., their continued existence in the presence of a local potential. We shall explore this in greater detail in the following section.

IV. SPIRALS IN THE PRESENCE OF INHOMOGENEITIES

This section is largely based on an earlier study of special types of solution of the NLKGE with a nonhomogeneous parameter.³³ The main assumption here is that the LG Hamiltonian in Eq. (5) may be adequate in the discussion of critical systems with defects provided the parameter A_2 is modified as follows:

$$A_2 = A/(2r^2), \quad (30)$$

so that the position of the defect is given by $r=0$. This may model both point-like defects and linear ones and can be of use in the context of polar elongated molecules present in the medium, such as is the case of microtubules or liquid crystals. The $1/r^2$ dependence is known to occur as the potential arising from a linear arrangement of electric dipoles. Within the framework of LG models position-dependent expansion parameters have been used in the past to model the presence of defects in crystals undergoing structural phase transitions³⁴ and more recently to include twin boundaries in the discussion of high-temperature superconductors.³⁵

We therefore postulate as our starting point, in the description of order-parameter dynamics in the vicinity of a defect, the following modified NLKGE:

$$\frac{\partial^2 \Phi}{\partial x_0^2} - \frac{\partial^2 \Phi}{\partial x_1^2} - \frac{\partial^2 \Phi}{\partial x_2^2} - \frac{\partial^2 \Phi}{\partial x_3^2} + Ar^{-2} \Phi + B_n \Phi^{n-1} = 0, \quad (31)$$

where the independent variables have been defined according to Eq. (8), with

$$B_n = 4A_4 \quad \text{for } n=4 \quad (32a)$$

and

$$B_n = 6A_6 \quad \text{for } n=6. \quad (32b)$$

We will be seeking anisotropic solutions in the form of spirals or helices which are allowed to move and rotate simultaneously with respect to a chosen axis x_3 . This type of solution takes the general form

$$\Phi = (x_1^2 + x_2^2)^a F \left[\omega x_0 - f(x_1^2 + x_2^2) - g(x_3 - vx_0) - \delta \sin^{-1} \frac{x_2}{(x_1^2 + x_2^2)^{1/2}} \right], \quad (33)$$

where a , f , g , v , and δ are to be fixed so that Φ of Eq. (33) will satisfy Eq. (31) self consistently. It can be established that two general classes of explicit solutions can be found depending on the form of F . The first class has been obtained assuming $F = f(r^2)$ is a constant with

$$r^2 = x_1^2 + x_2^2. \quad (34)$$

However, this case represents patterns which are neither spiral nor helical. A list containing several other functions of this type has been published in Ref. 32(b). On the other hand, we may also assume that $f(r^2) = 2\beta \ln r$ with $a = (n-2)^{-1}$. Then, it is found that the function g satisfies the two equations below:

$$(1-v^2)g'' = 0, \quad (\omega + vg')^2 - (g')^2 = 0. \quad (35)$$

Thus, g is a linear function of

$$\xi = \omega x_0 - f(r^2) - g(\xi) - \delta \theta \quad \text{with } \xi = x_3 - vx_0, \quad (36)$$

and the coefficient of proportionality clearly determines the relation between the rotational and translational velocities, ω and v , respectively. The equation on F is an autonomous ODE in the now familiar form of a damped

harmonic oscillator

$$(\delta^2 + 4\beta^2)F'' - 4a\beta F' + (4a^2 - A)F - B_n F^{n-1} = 0. \quad (37)$$

The reader is again referred to the Appendix. For $n=4$ and defining

$$\Delta = (4a^2 - A)/(\delta^2 + 4\beta^2), \quad S = -B_n/(\delta^2 + 4\beta^2) \quad (38a)$$

and

$$Q = -(4a\beta)/(\delta^2 + 4\beta^2) \quad (38b)$$

produces a class of exact solutions whenever $Q^2 = 9\Delta/2$ with $\Delta, S > 0$, which are given below:

$$F = C_1 \exp(-Q\xi) \operatorname{cn}[C_1 \lambda \exp(-Q\xi) + C_2; 1/\sqrt{2}], \quad (39a)$$

where

$$\lambda = 3S^{1/2}/(\sqrt{2}Q). \quad (39b)$$

In Eq. (39) C_1 and C_2 are arbitrary integration constants. A representative of this class of solutions is illustrated in Fig. 4. It is worth drawing the attention of the reader to the fact that certain arbitrariness in the choice of f , through the parameter β , and freedom in the choice of δ results in the possibility of forming spirals with various topological charges. In addition, certain choices of parameters, which describe amplitude and argument, will lead to discontinuities which would dramatically affect the pictorial representation of these spirals. In the Appendix, two other types of solution of Eq. (37) are presented.

When $\Delta < 0$, $S > 0$ and $Q^2 = -9\Delta/2$, another type of solution appears which may also give rise to spiral patterns. This takes the form

$$F = \left[\frac{-\Delta}{2S} \right]^{1/2} \left\{ 1 - \tanh \left[\left[\frac{-\Delta}{8} \right]^{1/2} (\xi - \xi_0) \right] \right\}, \quad (40)$$

and is a particular solution, there being only one integration constant ξ_0 appearing in Eq. (40).

In conclusion, we have shown that spiral and helical structures may arise due to the presence of low-dimensional defects, especially linear ones. This possibility *does not* crucially depend on whether or not the system

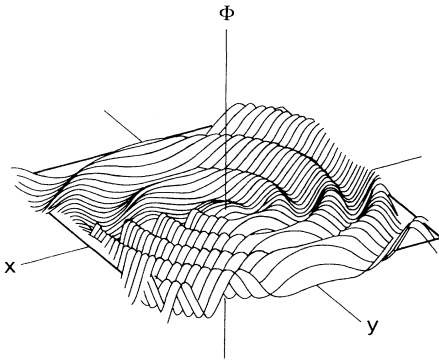


FIG. 4. Plot of the spiral wave based on the solution in Eq. (39) with topological charge equal to one.

is at the critical or tricritical point since the parameter A is arbitrary. Within our ansatz, however, it is imperative that the local potential due to the defect be proportional to $1/r^2$. For quintic nonlinearity in Eq. (37) a complete set of solutions can be obtained based on Eqs. (A20)–(A24) provided the parameters in Eq. (37) satisfy

$$A = \frac{1}{4} \left[1 - \frac{3}{4} \frac{\beta^2}{\delta^2 + 4\beta^2} \right]. \quad (41)$$

It should be noted that the solutions given by Eqs. (A20)–(A24) are not singular in view of the fact that the cn function oscillates between $+1$ and -1 .

V. AN APPLICATION TO SPIRAL DOMAIN STRUCTURES IN THIN FERROMAGNETIC FILMS

A. Background information

As already mentioned in the Introduction, several laboratories have observed the formation of spiral domains in uniaxial ferromagnetic thin films. Such an observation was made by Puchalska and Jouve⁸ and involved Sm-YIG garnets coated with permalloy layers of different thicknesses. Spiral domains were generated as a result of $n\pi$ -rotations of an in-plane magnetic field. Therefore, it is not surprising that such structures did develop since the in-plane field rotation induced the winding structure. A much more surprising result was the work by Kandaurova and Sviderskii,⁷ which reported the formation of spiral domains in the epitaxially-grown single garnet ferrite films. These spirals were formed when the film was subjected to an alternating square magnetic field along the easy magnetization axis normal to the plane. Moreover, a narrow amplitude range and a frequency threshold were necessary for the spirals to develop with $80 \leq H \leq 87$ Oe and frequency ≥ 300 Hz. The spiral domains were of macroscopic area (≈ 1 mm in diameter) and emerged following a destabilization of a typical labyrinthine domain structure and a subsequent complete randomization thereof. The lifetimes of the created spirals were substantial (≈ 10 s) and they persisted for as long as the external field was applied. Furthermore, the observed spiral domains exhibited soliton-like qualities of stability with respect to collisions between neighboring pairs.

In a later report, fascinating observations were reported in the same magnetic compound. These authors documented the occurrence of self-organizational processes in a system of moving spiral domains. They were able to produce quasiperiodic chainlike structures composed of spirals as well as nearly periodic lattices. The particular pattern selection was sensitive to the frequency, the amplitude, and level of uniformity of the magnetic field applied. One of the latest publications in this area⁶ claims the formation of spirals and their lattices, under equilibrium conditions, in the presence of a static magnetic field, provided special types of defects are present.

B. Solutions and their stability

We wish to address the question of spiral domain formation from a theoretical point of view. As usual, the simplest approach is to follow the LG model and propose the free energy expansion of the type

$$G = \int [A_2 M^2 + A_4 M^4 + A_6 M^6 - hM + \frac{1}{2}D(\nabla M)^2] dx dy \quad (42)$$

where M is the z component of the magnetization vector (along the easy-magnetization axis) and h is an external magnetic field in the same direction. This type of modeling is quite common for ferromagnetic films and multilayers.^{36–38} We have seen in the earlier sections of this paper that spiral solutions which minimize the free energy functional, with a density as in Eq. (42), exist in a strict sense only under a very specific set of circumstances.

(1) At the critical point, where $A_2 = A_6 = h = 0$, they can be found in the form

$$M(x, y) = \rho(x, y)F(\xi), \quad (43)$$

where

$$\xi = \frac{-2B}{B^2 + 1}(\theta + \frac{1}{2}B \ln r)$$

and

$$\rho = \left[\frac{4B^2}{|c|(B^2 + 1)r^2} \right]^{1/2}, \quad (44)$$

while F satisfies

$$F'' + F' + \frac{B^2 + 1}{4B^2}F - F^3 = 0. \quad (45)$$

Here, B is an arbitrary parameter, $\theta = \tan^{-1}(y/x)$, $r^2 = x^2 + y^2$, and c is given by $c = 4A_4/D$. Note that Eq. (45) has only one stable equilibrium point given by $F = 0$, $F' = 0$. Using a linearization procedure it is easy to find the corresponding eigenvalues as

$$\lambda_{\pm} = -\frac{1}{2} \pm \frac{1}{2} \sqrt{1 - (B^2 + 1)/B^2}.$$

Thus, for arbitrary values of B the eigenvalues are complex numbers and consequently the solution $F(\xi)$ is an oscillating function of its argument near $F = 0$. Therefore, the situation described by Eq. (45) can be classified as underdamped. However as $B \rightarrow \infty$, the expression under the square root (in λ_{\pm} , i.e., the imaginary part of eigenvalues tends to zero and the limiting case becomes critically damped with a corresponding lack of oscillatory behavior.

(2) At the tricritical point, where $A_2 = A_4 = h = 0$, the magnetization takes the same form as in Eq. (43). Here ξ is the same but ρ is given by

$$\rho = \left[\frac{4B^2}{|d|(B^2 + 1)r^2} \right]^{1/4}, \quad (46)$$

where d is given by $d = 6A_6/D$ and F satisfies

$$F'' + F' + \frac{B^2 + 1}{4B^2}F - F^5 = 0. \quad (47)$$

Clearly, the experiments described earlier do not seem to hinge on the proximity of the critical or tricritical points. What is important, however, is the crucial dependence of spiral formation on the amplitude of the alternating square magnetic field. The phenomenon seems to persist over a wide frequency range provided a threshold is exceeded (120–6000 Hz at least). In Fig. 5 we have schematically illustrated a possible scenario to explain the experimental results. In Fig. 5(a) we can see the effective on-site potential $V(M)$ as a function of temperature close to $T = T_c$. Note that it becomes flat-bottomed at $T = T_c$. Figure 5(b) shows that the same type of effect takes place at the tricritical point $T = T_t$. What we have attempted to convey in Fig. 5(c) is that the alternating square magnetic field may mimic the flat-bottoming character of the potential curve provided the frequency of alternation of the field is high compared with the relaxation frequency of the collective modes of the strongly interacting spin system τ^{-1} , so that $\omega \gg \tau^{-1}$. Under these conditions, the system residing initially in the disordered phase $M = 0$ (grey background referred to in Ref. 4), never has the chance to relax to its instantaneous equilibrium at the bottoms of the double well. With a proper balance between expansion coefficients A_2 , A_4 , and A_6 on the one

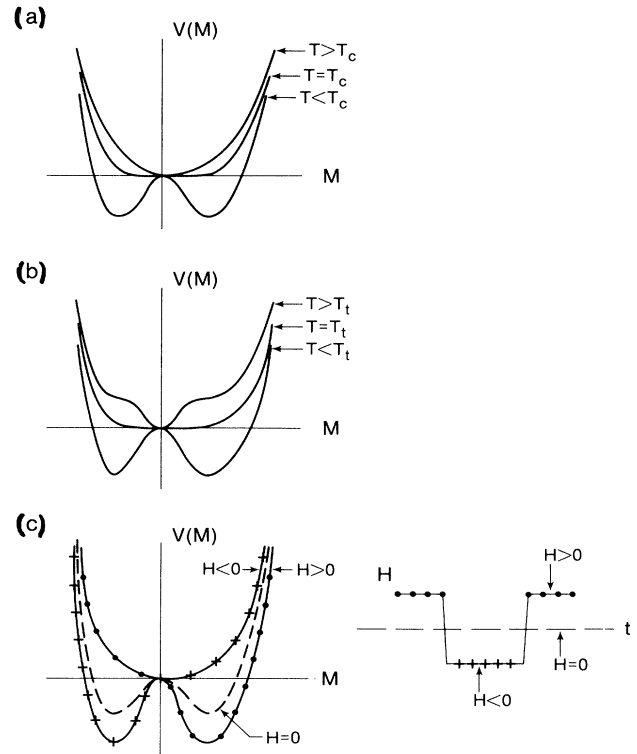


FIG. 5. (a) The effective on-site potential $V(M)$ as a function of temperature close to T_c ; (b) $V(M)$ as a function of T close to T_t and; (c) the situation in the presence of an alternating square magnetic field.

hand, and the magnetic field on the other, the effective potential “seen” by the spin system is composed of the two top branches for each half-period. This gives the effective free energy density as

$$G = A_2 |M|^2 + A_4 |M|^4 + |h| |M| + (D/2)(\nabla M)^2. \quad (48)$$

This can be translated into a condition between the magnetic field h and the temperature as

$$|h| \simeq -A_2 |M|. \quad (49)$$

We have analyzed this requirement on $|h|$ and shown it to correspond to the disappearance of the mean-field part of the free energy which results from the application of h , occurring for magnetization ranging between 57% and 62% of equilibrium magnetization. It is well known that, since $A_2 = \alpha(T - T_c)$ according to Landau theory, close to $T = T_c$, magnetization scales as $M \sim (T - T_c)^{1/2}$, giving rise to the relationship on the amplitude of the field required for spiral formation, as

$$|h| \sim (T - T_c)^{3/2}, \quad (50)$$

with a precisely specified amplitude prefactor due to the condition discussed above. In this connection we wish to emphasize the amplitude value and not just the critical exponent of $\frac{3}{2}$ which is standard in such situations. Based on this result, we can predict that the lowering of the temperature in this type of experiment would require a larger amplitude of the field in order to produce spirals and this amplitude would have to be proportional to $|T - T_c|^{3/2}$ for this to take place. Destroying this delicate balance causes a departure from the flat-bottom situation which, in turn, permits the nucleation of homogeneous domains of one phase. It should also be noted that having the local minimum of the effective potential at $M = 0$ appears favorable from the point of view of slow relaxation times for collective spin dynamics.

C. Energy calculations

The next property we wish to explore is the energy expense needed to form a spiral domain with N_0 turns. An exact calculation is, at the present time, not feasible since solutions to Eqs. (45) and (47) are known only for particular values of the constant B and even then take the form of very complicated special functions. However, in Fig. 6, following the discussion below Eq. (45), we have shown a typical dependence of F on ξ for such an equation which indicates a rather rapid damping as a function of ξ . Therefore, we propose an approximate method which represents F as a rectangle of width w and height F_0 , with F_0 being the space- and time-independent (constant) solution of Eqs. (45) and (47), i.e.,

$$F_0 = \left[\frac{B^2 + 1}{4B^2} \right]^{1/(n-2)}, \quad (51)$$

where $n = 4$ or 6 for the two cases. With this approximation and the damping due to the presence of ρ in $M(\xi)$, along the direction normal to the spiral, we calculate the energy to form a spiral as

$$\Delta E = \int_A \int [A_2 M^2 + A_4 M^4 + A_6 M^6 + \frac{1}{2} D (\nabla M)^2] r dr d\theta, \quad (52)$$

where A is the area traced out by the spiral when $F \neq 0$. Here, we take M as

$$M(\xi) = [c|r^2]^{-1/2}, \quad (53)$$

at the critical point and

$$M(\xi) = [d|r^2]^{-1/4}, \quad (54)$$

at the tricritical point. These expressions are taken to be valid within the width w along the length of the spiral. The latter implies the following parametrization:

$$r = r_0 \exp \left[\frac{-2}{B} \theta \right], \quad (55)$$

where r_0 is found to be

$$r_0 = \exp \left[\frac{-(B^2 + 1)\xi_0}{B^2} \right], \quad (56)$$

and ξ_0 is the chosen value of the symmetry variable. The free parameter B can be deduced from the pitch of the spiral when actual modeling is done. For the critical point, the results are

$$\Delta E = -w \left[A_4 m^2 + \frac{D}{2} \right] m^2 r_0^{-2} \frac{B^2 + 1}{8|B|} \times \left[1 - \exp \left[\frac{-8\pi N_0}{|B|} \right] \right], \quad (57)$$

where m in this case is $m = F_0 |c|^{-1/2}$. For the tricritical point we find

$$\Delta E = -w \left[A_6 \bar{m}^4 + \frac{D}{8} \right] \bar{m}^2 r_0^{-1} \frac{B^2 + 1}{4|B|} \times \left[1 - \exp \left[\frac{-4\pi N_0}{|B|} \right] \right], \quad (58)$$

where \bar{m} is defined by

$$\bar{m} = F_0 |d|^{-1/4}. \quad (59)$$

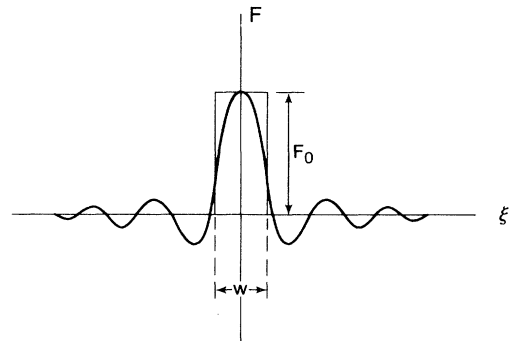


FIG. 6. Graphical illustration of the approximation used for $F = F(\xi)$.

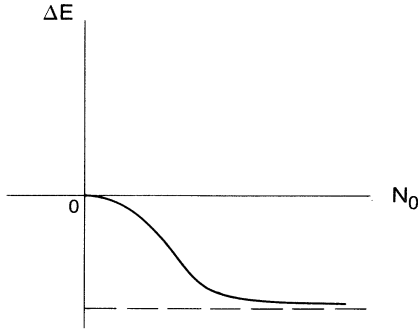


FIG. 7. Plot of ΔE as a function of N_0 for spiral patterns as in Eqs. (57) and (58).

Figure 7 illustrates the dependence of ΔE on N_0 as given by Eqs. (57) and (58). The spirals which we have described here are expected to arise at $T=T_c$ or at the tricritical point $T=T_t$, and persist for a range of temperatures below the two. Since the spiral profile represents nucleation of the ordered phase, the energies calculated in Eqs. (57) and (58) have a negative sign as energetically favorable compared to the disordered background (which is set at the zero energy) against which the spiral is formed. However, the entire pattern requires our energy input to sustain *both* the spiral and the background surrounding it. We therefore, have to estimate this latter contribution separately. This is calculated as the approximate area swept out by the spiral arm multiplied by the energy density of a mean-field disordered background. Thus,

$$\Delta E' = \pi R^2 \varepsilon, \quad (60)$$

where R is the outer radius corresponding to the last turn and ε is the mean background energy density. It is relatively easy to find the value of ε as

$$\varepsilon_c = A_2^2 / (4A_4), \quad (61)$$

for temperatures close to $T=T_c$, while

$$\varepsilon_t = |9A_2 A_4 A_6 - 2A_4^3 \pm 2(A_4^2 - 3A_2 A_6)^{3/2}| / (27A_6^2), \quad (62)$$

for temperature close to $T=T_t$. Note that in the first case ε_c scales with $(T-T_c)^2$ while in the second case this type of scaling is not so easy to describe by a power law. The total energy of the spiral pattern, therefore, is given by

$$E = \Delta E + \Delta E'. \quad (63)$$

The background energy as a function of the angle variable θ is then

$$\Delta E' = \varepsilon \pi e^{4\theta/|B|}. \quad (64)$$

Thus, for N_0 windings we may write

$$\Delta E' = \Delta \exp(\bar{\alpha} N_0), \quad (65)$$

and

$$\Delta E = -\delta [1 - \exp(-\bar{\alpha} N_0)], \quad (66)$$

where Δ , $\bar{\alpha}$ and δ are defined by Eqs. (64) and (62) [or (57)], respectively. Note that all of these parameters take different values at critical and tricritical points. In Fig. 8 we schematically illustrate the radial dependence of ΔE and $\Delta E'$ as a function of R and θ . The total energy exhibits a definite minimum at $R=\bar{R}$. The calculation of \bar{R} and the fluctuations about it will be given later in this section.

D. Statistical properties

We would like to carry out statistical calculations for assemblies of such spiral patterns. First, the partition function can be evaluated as

$$Z \simeq e^{-\beta \delta} \int_0^\infty e^{-\beta \Delta \exp(\bar{\alpha} N_0)} [1 - \beta \delta \exp(-\bar{\alpha} N_0)] dN_0. \quad (67)$$

The integral in Eq. (67) can be evaluated approximately by expanding the third term in the exponential so that

$$Z \simeq e^{\beta \delta} \int_0^\infty e^{-\beta \delta \exp(\bar{\alpha} N_0)} [1 - \beta \delta \exp(-\bar{\alpha} N_0)] dN_0. \quad (68)$$

This approach is well justified due to the relative smallness of the spiral energy compared to its background, particularly for large winding numbers. We now use

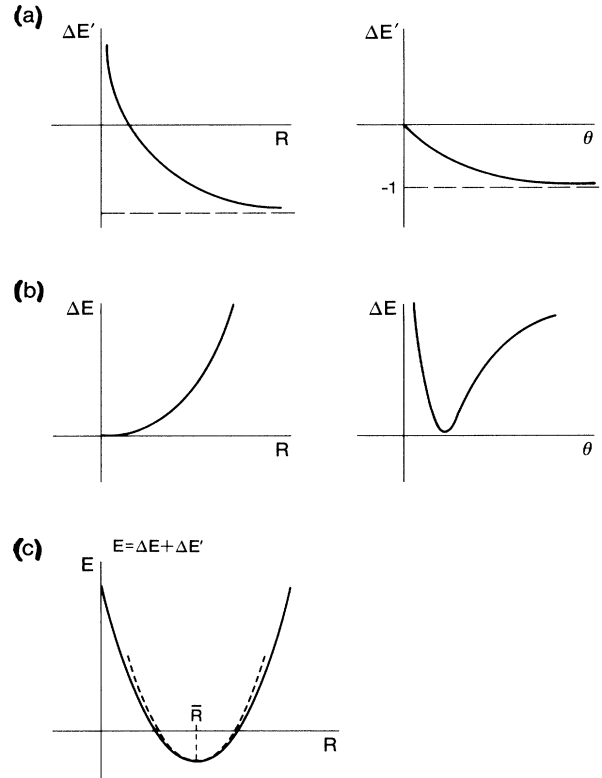


FIG. 8. Plots of (a) ΔE ; (b) $\Delta E'$ as functions of R and θ ; and (c) the dependence of the total energy of a spiral E on its size R .

standard formulas³⁹ to evaluate Eq. (68) to give

$$Z \simeq e^{\beta\delta} \left[\frac{-1}{\bar{\alpha}} \text{Ei}(-\beta\Delta) - \frac{\delta\beta^2}{\bar{\alpha}} \Delta\Gamma(+1, \beta\Delta) \right], \quad (69)$$

where Ei is the exponential integral function and Γ is the incomplete gamma function. An approximate formula can also be found for the average number of windings of a spiral using

$$\langle N_0 \rangle = \int_0^\infty N_0 e^{-\beta E} dN_0 / Z \simeq Z^{-1} \int_0^\infty (e^{N_0} - 1) e^{-\beta\Delta \exp(\bar{\alpha}N_0)} [1 - \beta\delta \exp(-\bar{\alpha}N_0)] dN_0, \quad (70)$$

where we have used the same approximation as in Eq. (68), for Z , and made use of a series expansion for the exponential function. The final result is

$$\langle N_0 \rangle = \left[(\beta\Delta)^{-1/\bar{\alpha}} \Gamma\left(\frac{1}{\bar{\alpha}}, \beta\Delta\right) - \delta\beta(\Delta\beta)^{(\bar{\alpha}-1)/\bar{\alpha}} \Gamma\left(\frac{1-\bar{\alpha}}{\bar{\alpha}}, \beta\Delta\right) - \bar{\alpha}Z \right] / \bar{\alpha}Z. \quad (71)$$

It can be found that for *high temperatures* or $\beta \rightarrow 0$, the mean number of turns will vanish as expected. A similar inspection of the asymptotic limit, $\beta \rightarrow \infty$, or *low temperatures*, shows a similar type of behavior. Thus, there appears to be a range of *intermediate temperatures* in which spirals are most likely to arise. The formula (71), however, is too complicated to provide simple answers as to the temperature dependence of the number of turns.

In this final part of this section we will provide another insight into the size distribution of spiral patterns using a minimization method. The starting point is to write the energy of a spiral pattern in terms of its radius only, i.e.,

$$E = \pi\epsilon R^2 - \delta(1 - r_0^2/R^2). \quad (72)$$

Minimizing E with respect to R yields the most probable radius, \bar{R} , as

$$\bar{R} = \left[\frac{\delta r_0^2}{\pi\epsilon} \right]^{1/4}. \quad (73)$$

This quantity diverges as $T \rightarrow T_c$, since $\epsilon \sim (T - T_c)^2$. This would indicate high likelihood of the occurrence of large spirals close to $T = T_c$ (where it is energetically inexpensive to sweep a large area of disordered background). As the temperature is lowered, below $T = T_c$, the energy associated with the disordered background increases, giving rise to a shrinkage of the spiral. However, an important aspect in this connection is the average fluctuation in the mean radius, i.e., $(R - \bar{R})^2$, which is inversely proportional to the curvature of $E(R)$. That is,

$$\overline{(R - \bar{R})^2} \sim \left[\frac{d^2 E}{dR^2} \right]^{-1}. \quad (74)$$

It is easy to evaluate this latter quantity and we find

$$\frac{d^2 E}{dR^2} = 8\pi\epsilon. \quad (75)$$

As a result, the magnitude of fluctuations relative to the most probable radial size is given by

$$\left[\frac{\overline{(R - \bar{R})^2}}{\bar{R}^2} \right]^{1/2} \sim \epsilon^{-1/4}. \quad (76)$$

Thus, the fluctuations in size distribution are even larger

than the mean size of the spiral as $T = T_c$ is approached. Assuming that the energy of the spiral ΔE is proportional to the number of its arms leads to the conclusion that the magnitude of fluctuations relative to the most probable radial size scales with the topological charge raised to the power $-\frac{1}{4}$. We hope that the results provided in this part of our analysis will be of use in future direct comparisons with experiment.

VI. CONCLUSIONS

In this paper we have provided an overview of recent experimental observations which indicate a widespread appearance of spiral order-parameter structures. More importantly, we have attempted to provide a unified theoretical framework within which spiral patterns arise as exact solutions. The formalism used was that of an LG model, which in view of recent studies, is much less phenomenological than it has been thought hitherto. It was demonstrated that spirals can be found as exact solutions to a number of generic equations of motion provided the latter ones possess scaling properties. In physical terms this implied the immediate proximity of either the critical or tricritical points. This condition appears too restricted perhaps, but indeed, in Sec. IV, we have shown another avenue through which spirals can come into being. The presence of defects producing singular potential curves was shown to lead to the creation of helical and spiral patterns. Thus, defects can be thought of as nucleation centers for the appearance of spiral domains.

In the final section an in-depth analysis was given of spiral domain structures in thin ferromagnetic films. First of all, it was argued that experimental conditions requiring the presence of an alternating square magnetic field of a particular amplitude, played the role of an effective mean-field potential at criticality or tricriticality, on the scale of the relaxation time. Extreme sensitivity to the amplitude of the applied field and lack of dependence on a wide range of frequencies seem to support that statement. We then obtained approximate expressions for the energy stored in a spiral pattern together with its background and used these expressions to calculate the partition function and other statistical quantities. An important qualitative result was obtained which indicates that the average size of a spiral increases unboundedly as T

approaches $T = T_c$ from below, but such is also the case for the magnitude of size fluctuations. Due to the large amount of fluctuation, one expects assemblies of spirals to exhibit substantial variation and irregularity as has been observed experimentally for thin films. We intend to continue this research in the near future with the intention of providing direct quantitative comparison with experiment.

ACKNOWLEDGMENTS

This research has been supported by Grants from the Natural Sciences and Engineering Research Council of Canada and NATO. One of us (J.M.D.) would like to thank the Faculty members and staff of the Department of Physics for their hospitality and kindness during his stay at the University of Alberta. The authors are very grateful to Dr. M. Skierski for providing many useful references to spiral structures.

APPENDIX

In this appendix we present a selection of solutions for damped anharmonic oscillator equations of the form

$$F'' + \gamma F' = P(F), \quad (\text{A1})$$

where $P(F)$ denotes a polynomial in the dependent variable F , the independent coordinate being ξ in each case. In each case we give the form of $P(F)$ and the source from which it arises. The symbols A , B , and C below denote constants which are not arbitrary, but have to be carefully chosen for each solution.

1. Solutions in terms of elementary functions

a. The Chan solution (Ref. 40): $P(F) = AF + BF^2 + CF^3$

The particular solution in this case is

$$F = F_3 [1 + \exp(F_3 \sqrt{C/2\xi})]. \quad (\text{A2})$$

Here F_1 , F_2 , and F_3 are the roots of $P(F) = 0$, namely

$$F_1 = 0 \quad \text{and} \quad F_2, F_3 = -\frac{1}{2C} (B \mp \sqrt{B^2 - 4AC}). \quad (\text{A3})$$

This solution only exists provided the damping constant γ is given by

$$\gamma = -\frac{1}{4} \sqrt{2/C} (3\sqrt{B^2 - 4AC} - B^2). \quad (\text{A4})$$

b. The Montroll (Ref. 41) and Metiu, Kitahara and Ross (Ref. 42) result:
 $P(F) = a(F - F_1)(F - F_2)(F - F_3)$

One solution here may be written as

$$F = F_1 + (F_3 - F_1) [1 + \exp(\mu\xi)]^{-1}, \quad (\text{A5})$$

where $\mu = \pm(F_3 - F_1)\sqrt{a/2}$; a is a constant. The stipulation on γ that (A5) be a solution is

$$\gamma = \mp \sqrt{2a} (F_3 + F_1 - 2F_2). \quad (\text{A6})$$

c. Solution due to Cerveró and Estévez (Ref. 43): $P(F) = F^3 - F$

When the dissipation factor $\gamma = 3/\sqrt{2}$, a kink solution can be found in the form

$$F = \mp \frac{1}{2} \{1 - \tanh[(1/2\sqrt{2})(\xi - \xi_0)]\}, \quad (\text{A7})$$

where ξ_0 is an integration constant.

d. The Gordon (Ref. 44) solution for quintic nonlinearity: $P(F) = AF + CF^3 + EF^5$

In this case a kinklike solution was found taking the form

$$F = F_1 [1 + \exp(-\mu\xi)]^{-1/2}, \quad (\text{A8})$$

where F_1 is a root of the quintic $P(F)$ corresponding to a global minimum of the underlying potential energy.⁴⁴ The constant μ is an elaborate function of the constants A , C , and E , and for Eq. (A8) to be a solution these constants must be related in a special way. The reader may obtain further details from the original source.⁴⁴

e. The Parliński and Zieliński solution (Ref. 45):
 $P(F) = AF + BF^{n+1} + CF^{2n+1}$

Here, n denotes an integer. Their exact kinklike solution is

$$F = F_0 \{1 + \exp[\nu(\xi - \xi_0)]\}^{-1/n}. \quad (\text{A9})$$

There is a consistency condition among the parameters F_0 , ν , A , B , and C for this to be a solution but ξ_0 is an arbitrary constant. These authors also found an approximate solution, in the asymptotic limit $\xi \rightarrow \mp \infty$, composed of a pair of solutions like that in Eq. (A9), namely

$$F = F_0^2 \{1 + \exp[\nu(\xi - \xi_0)]\}^{-1/n} \times \{1 + \exp[-\nu(\xi - \xi_1)]\}^{-1/n}, \quad (\text{A10})$$

where ξ_0 and ξ_1 are constants.

f. A solution due to Hereman and Takaoka (Ref. 46) [and Wang (Ref. 47)]: $P(F) = F(F^c - 1)$

Solutions were discovered independently by the two sets of authors and c is an arbitrary real number. They found that

$$F = 2^{-2/c} \left\{ 1 - \tanh \left[\left[\frac{c}{2\sqrt{2c+4}} \right] (\xi - \xi_0) \right] \right\}^{2/c}, \quad (\text{A11})$$

where ξ_0 is an arbitrary constant and $\gamma = -(c+4)/\sqrt{2c+4}$.

g. Solutions found by Otwinowski, Paul, and Laidlaw (Ref. 48)

1. $P(F) = A_1 - A_2 F + A_4 F^3$. Three bounded solutions

$$F(\xi) = \frac{1}{2a_4} [\text{sgn}(a_2^{(i)} a_4) \sqrt{\Delta_i} \tanh(\frac{1}{2} \sqrt{\Delta_i} \xi) - a_2^{(i)}], \quad i = 1, 2, 3 \quad (\text{A12})$$

have been found for $|A_1| \leq (-\frac{4}{27}A_4^{-1}A_2^3)^{1/2}$, where $A_2^{(i)}$ is one of the three roots of the cubic equation

$$a_2^3 + \frac{A_2}{2}a_2 + \frac{A_1}{2}a_4 = 0,$$

and

$$a_4 = \pm(\frac{1}{2}A_4)^{1/2}, \quad a_0^{(i)} = -\frac{A_1}{2a_2^{(i)}},$$

$$\Delta_i = (a_2^{(i)})^2 - 4a_0^{(i)}a_4.$$

The damping coefficient must satisfy $\gamma = -3a_2^{(i)}$.

2. $P(F) = A_2 F + A_4 F^3 + A_6 F^5$. A solution is found by the authors⁴⁸ in the form

$$F = F_0 \{1 + \exp[\nu(\xi - \xi_0)]\}^{-1/2}, \quad (\text{A13})$$

F_0 being a constant amplitude and ξ_0 an arbitrary constant.

3. $P(F) = A_2 F + A_3 F^2$. Provided the damping constant is given by

$$\gamma = \mp 5\sqrt{-A_2/6}, \quad (\text{A14})$$

a solution may be found of the form⁴⁸

$$F = -\frac{2A_2}{A_3} \{1 + \exp[\mp \sqrt{-A_2/6}(\xi - \xi_0)]\}^{-2}. \quad (\text{A15})$$

h. Dixon, Tuszyński, and Otwinowski solutions:

$$P(W) = W^{n-1} - AW \text{ and } \gamma = 1$$

(i) For $A = \frac{2}{9}$ and $n=4$ a kink solution is found and is given by

$$F = \mp \sqrt{A} / \{1 + \exp[\pm \sqrt{A}(\xi - \xi_0)]\}. \quad (\text{A16})$$

(ii) When $A = \frac{3}{16}$ with $n=6$ the authors²⁷ find

$$F = -\left[\frac{4}{\sqrt{3}} \{1 + \exp[\mp \frac{1}{2}(\xi - \xi_0)]\} \right]^{-1/2}. \quad (\text{A17})$$

In Eqs. (A2), (A5), (A7), (A12) and (A16) solutions are seen to take the form of a ratio of linear combinations of exponentials, i.e., which may be written as

$$F = [\lambda_1 \exp(\alpha \bar{\xi}) + \lambda_2 \exp(-\alpha \bar{\xi}) + \lambda_3] \times [\lambda_4 \exp(\alpha \bar{\xi}) + \lambda_5 \exp(-\alpha \bar{\xi}) + \lambda_6]^{-1}, \quad (\text{A18})$$

where $\bar{\xi} = \xi - \xi_0$, ξ_0 being arbitrary and λ_i ($i=1-6$) and

α are constants to be adjusted.

2. Solutions in terms of elliptic functions:

Cases with $P(F) = \lambda F + \mu F^n$

where λ and μ are fixed constants

$$a. P(F) = -\frac{2}{9}F + F^3: \gamma = 1$$

This special form of equation satisfies the Painlevé criterion and the general class of nonsingular solutions take the form

$$F(\xi) = \mp \frac{1}{2}c_1 \exp(\frac{1}{3}\xi) \text{sd}\{\sqrt{2}[c_1 \exp(\frac{1}{3}\xi) + c_2], 1/\sqrt{2}\}. \quad (\text{A19})$$

Here, c_1 and c_2 are arbitrary integration constants and sd is the Jacobi elliptic function $\text{sd} = \text{sn}/\text{dn}$ with the elliptic modulus $k=1/\sqrt{2}$. Cerveró and Estévez⁴³ found an analogous solution with a ds rather than an sd solution. Note that the solution in Eq. (A19) is nonsingular whereas the one with ds replacing sd has an infinite number of divergent points.

$$b. P(F) = -\frac{3}{16}F + F^5: \gamma = 1$$

The solution here is written in the form

$$F = \lambda \left[\frac{\sqrt{3}}{4} \xi \right] u(s), \quad (\text{A20})$$

where

$$s = -\frac{\sqrt{3}}{2} \left[\frac{c_2}{c_1} \right]^2 \exp\left[-\frac{2}{\sqrt{3}} \xi \right] \quad (\text{A21})$$

and

$$u = \left[\frac{3c_3}{c_1} \right]^{1/6} \left[\frac{\text{cn}(z, k) - 1}{(1 - \sqrt{3})\text{cn}(z, k) + (1 + \sqrt{3})} \right]^{1/2} \quad (\text{A22})$$

with

$$z = (3)^{1/4} \sqrt{4c_3} \left[\frac{c_1}{3c_3} \right]^{1/6} (\xi - \xi_0). \quad (\text{A23})$$

In Eq. (A23) ξ_0 is an arbitrary constant and the Jacobi modulus k is given by

$$k = \left[\frac{2 - \sqrt{3}}{4} \right]^{1/2}. \quad (\text{A24})$$

¹H. Müller-Krumbhaar, in *Fluctuations, Instabilities and Phase Transitions*, edited by T. Riste (Plenum, New York, 1975).

²T.F. Braish, J. C. Sandler, and P. L. Fuchs, *J. Org. Chem.* **53**, 3647 (1988).

³D. C. Mattis, *The Theory of Magnetism* (Springer, Berlin, 1981).

⁴G. S. Kandaurova and A. E. Sviderskii, *Pis'ma Zh. Eksp. Teor. Fiz.* **47**, 410 (1988) [*JETP Lett.* **47**, 490 (1988)].

⁵J. A. Tuszyński, in *The Spring Symposium Proceedings of MRS*,

edited by E. E. Marinero MRS Symposia Proceedings No. 151 (Materials Research Society, Pittsburgh, 1989), p. 265.

⁶A. P. Ges, V. V. Fedotova, A. K. Bogush, and T. A. Gorbachevskaya, *Pis'ma Zh. Eksp. Teor. Fiz.* **52**, 1079 (1990) [*JETP Lett.* **52**, 476 (1990)].

⁷G. S. Kandaurova and A. E. Sviderskii, *Zh. Eksp. Teor. Fiz.* **97**, 1218 (1990) [*Sov. Phys. JETP* **70**, 684 (1990)].

⁸I. B. Puchalska and H. Jouve, *IEEE Trans. Magn.* **MAG-13**, 1178 (1977).

- ⁹J. M. Ziman, *Models of Disorder* (Cambridge University Press, Cambridge, 1979).
- ¹⁰A. Joets and R. Ribotta, *J. Phys. (Paris)* **47**, 595 (1986).
- ¹¹For an extensive review see A. T. Winfree *SIAM Rev.* (to be published); and also A. T. Winfree, *The Geometry of Biological Time* (Springer-Verlag, New York, 1990).
- ¹²(a) K. I. Agladze, V. A. Davydov, and A. S. Mikhailov, *Pis'ma Zh. Eksp. Teor. Fiz.* **45**, 601 (1987) *JETP Lett.* **45**, 767 (1987); (b) K. I. Agladze, V. I. Krinsky, A. V. Panfilov, H. Linde, and L. Kuhnert, *Physica D* **39**, 38 (1989); (c) V. I. Krinskii and K. I. Agladze, *Dokl. Akad. Nauk SSSR* **263**, 335 (1982) [*Sov. Phys. Dokl.* **27**, 228 (1982)].
- ¹³J. J. Hegseth, C. D. Andereck, and Y. Pomeau, *Phys. Rev. Lett.* **62**, 257 (1989).
- ¹⁴(a) J. D. Murray, *Mathematical Biology* (Springer, Berlin, 1989); (b) N. Kopell and L. N. Howard, *Stud. Appl. Math.* **52**, 291 (1973).
- ¹⁵M. A. Gorman, M. el-Hamdi, K. A. Robbins, in *Nonlinear Structures in Physical Systems*, edited by L. Lam and H. C. Morris (Springer, Berlin, 1989).
- ¹⁶K. Vos, J. M. Dixon, and J. A. Tuszyński, *Phys. Rev. B* (to be published).
- ¹⁷J. J. Tyson and J. P. Keener, *Physica D* **32**, 327 (1988).
- ¹⁸C. Henze, E. Lugosi, and A. T. Winfree, *Can. J. Phys.* **68**, 683 (1990).
- ¹⁹A. D. Linde, *Rep. Prog. Phys.* **42**, 389 (1979); G. Berlin and J. W.-K. Mark, *SIAM J. Appl. Math.* **36**, 407 (1979).
- ²⁰Y. Bouligand, in *Physics of Defects*, Les Houches Session XXXV, edited by R. Balian, M. Kléman, and J.-P. Poirier (North-Holland, Amsterdam, 1981).
- ²¹L. D. Landau and E. M. Lifshitz, *Statistical Mechanics* (Pergamon, Oxford, 1969).
- ²²(a) J. A. Tuszyński and J. M. Dixon, *J. Phys. A* **22**, 4877 (1989); (b) J. M. Dixon and J. A. Tuszyński, *ibid.* **22**, 4895 (1989); (c) J. A. Tuszyński and J. M. Dixon, *Phys. Lett. A* **140**, 179 (1989).
- ²³L. P. Gor'kov, *Zh. Eksp. Teor. Fiz.* **36**, 1918 (1959) [*Sov. Phys. JETP* **9**, 1364 (1959)].
- ²⁴P. J. Olver, *Applications of Lie Groups to Differential Equations* (Springer, Berlin, 1986).
- ²⁵P. Winternitz, in *Partially Integrable Evolution Equations in Physics*, edited by R. Conte and N. Boccara (Kluwer Academic, Dordrecht, 1990).
- ²⁶P. Winternitz, A. M. Grundland, and J. A. Tuszyński, *J. Phys. C* **21**, 4931 (1988).
- ²⁷J. M. Dixon, J. A. Tuszyński, and M. Otwinowski, *Phys. Rev. A* (to be published).
- ²⁸P. Winternitz, A. M. Grundland, and J. A. Tuszyński, *J. Math. Phys.* **28**, 2194 (1987).
- ²⁹J. A. Tuszyński, M. Otwinowski, R. Paul, and A. P. Smith, *Phys. Rev. B* **36**, 2190 (1987).
- ³⁰(a) L. Gagnon and P. Winternitz, *J. Phys. A* **21**, 1493 (1988); (b) *Phys. Lett.* **134**, 276 (1989); (c) *Phys. Rev. A* **39**, 296 (1989).
- ³¹M. Skierski, A. M. Grundland, and J. A. Tuszyński, *Phys. Lett. A* **133**, 213 (1988); *J. Phys. A* **22**, 3789 (1989).
- ³²J. M. Greenberg, *SIAM J. Appl. Math.* **30**, 199 (1976).
- ³³(a) M. Otwinowski, R. Paul, and J. A. Tuszyński, *Can. J. Phys.* **68**, 756 (1990); (b) M. Otwinowski, in *Nonlinear Structures in Physical Systems*, edited by L. Lam and H. C. Morris (Springer, Berlin, 1990).
- ³⁴I. O. Mayer and A. I. Sokolov, *Jpn. J. Appl. Phys.* **24**(2), 185 (1985).
- ³⁵(a) A. M. Campbell, *Physica C* **162-164**, 273 (1989); (b) Yu. A. Danilov and V. I. Safonov, *Physica C* **153-155**, 683 (1988).
- ³⁶K. Binder and P. C. Hohenberg, *Phys. Rev. B* **6**, 3461 (1972).
- ³⁷D. Schwenk, F. Fishman, and F. Schwabl, *Phys. Rev. B* **38**, 11 618 (1988).
- ³⁸P. A. Dowben, D. LaGraffe, Dongqi Li, A. Miller, and Ling Zhang, *Phys. Rev. B* **43**, 3171 (1991).
- ³⁹I. S. Gradshteyn and I. M. Ryzhik, *Table of Integrals Series and Products* (Academic, New York, 1965).
- ⁴⁰S.-K. Chan, *J. Chem. Phys.* **67**, 5755 (1978).
- ⁴¹F. W. Montroll, in *Statistical Mechanics*, edited by S. A. Rice, K. F. Freed, and J. C. Light (University of Chicago Press, Chicago, 1972).
- ⁴²H. Metiu, K. Kitahara, and J. Ross, *J. Chem. Phys.* **64**, 292 (1976).
- ⁴³J. M. Cerveró and P. G. Estévez, *Phys. Lett. A* **114**, 435 (1986).
- ⁴⁴A. Gordon, *Phys. Lett.* **99A**, 329 (1983).
- ⁴⁵K. Parliński and P. Zieliński, *Z. Phys. B* **44**, 317 (1981).
- ⁴⁶W. Hereman and M. Takaoka, *J. Phys. A* **23**, 4805 (1990).
- ⁴⁷X. Y. Wang, *Phys. Lett. A* **131**, 277 (1988).
- ⁴⁸M. Otwinowski, R. Paul, and W. G. Laidlaw, *Phys. Lett. A* **128**, 483 (1988).